Desalination and Water Treatment
www.deswater.com
doi: 10.1080/19443994.2013.826775

52 (2014) 1028–1034
January

Taylor & Francis
Taylor & Francis Group

Effect of flux fluctuation on the fouling in membrane water treatment system for smart water grid

Suhan Kim[a,*], Jae-Lim Lim[b], Jong-Yul Park[c], Jong-Oh Kim[d]

[a]*Department of Civil Engineering, Pukyong National University, Yongdang-Dong, Nam-Gu, Busan, Korea Tel. +82-51-629-6065; Fax: 82-51-629-6063; email: suhankim@pknu.ac.kr*
[b]*Water Management & Research Center, K-water Institute, Jeonmin-Dong, Yusong-Gu, Daejeon, Korea*
[c]*Metawater Seoul Office, Sinmunno, Jongno-Gu, Seoul, South Korea*
[d]*Department of Civil Engineering, Gangneung-Wonju National University, Gangneung, Gangwon-do, South Korea*

Received 23 February 2013; Accepted 18 March 2013

ABSTRACT

Smart water grid is a water network with communication to save water and energy. In smart water grid, decentralized water management system is more suitable than the conventional centralized system. Membrane process can be a potent option of water treatment system for decentralized water management system due to stable product water quality regardless of periodic changes in water production rate (flux fluctuation) to meet a real-time water demand. In this study, the effect of flux fluctuation on membrane fouling was investigated using a simple microfiltration (MF) fouling model for field application. The fouling model was verified by operation data of a pilot-scale MF plant with two commercial MF membrane modules (72 m^2 of membrane area). From the MF simulation results, we found that periodic change in flux can induce higher fouling than the constant flux and the fouling becomes more severe as the range of the fluctuation increases. It was also found that the frequency of flux fluctuation was not related to fouling, if the average flux and the fluctuation range were not changed. Therefore, the range of flux fluctuation should be carefully designed when flux fluctuation in inevitable in membrane water treatment for smart water grid.

Keywords: Smart water grid; Membrane water treatment system; Flux fluctuation; Membrane fouling; Field application

1. Introduction

The concept of smart water grid is originated from smart grid for electricity [1]. Smart water grid can be defined as a water network that can cost-efficiently integrate the behavior and actions of all users connected to it (e.g. water supplier, consumers and those who do both) in order to ensure an economically efficient, sustainable water system with low losses and high levels of quality and security of supply and safety [2].

*Corresponding author.

Presented at the Fifth Annual International Conference on "Challenges in Environmental Science & Engineering—CESE 2012" Melbourne, Australia, 9–13 September 2012

Smart water grid needs an effective communication between each node to save water and energy, for example, water source, water treatment plant (WTP), pipe network, wastewater treatment plant, customers, water reuse and environment as seen in Fig. 1. The information for the inter communications are amount of source water, water flow rate, water quality, demand patterns, water price, environmental regulation, system availability and failure. In smart water grid, water suppliers can obtain an optimal supply strategy to meet a real-time water demand and customers easily get the information of water usage pattern coupled with variable water prices according to peak and ordinary time. The key technologies for smart water grid are smart water sensors, real-time water demand prediction, and optimization [2].

Decentralized water management system is more beneficial than the centralized system for effective communication and feedback between nodes in smart water grid. Water demands of smaller (decentralized) customer groups are much easier to be predicted than those of larger groups, because water demand pattern is variable according to the customer types (e.g. various residential types, industry, business/shopping district, and agricultural areas). In addition, decentralized water management system can be regarded as the appropriate approach for smart water grid when water reuse option is considered for saving more water resources [3].

Smaller WTP is more preferred in decentralized water management system, and the change in water production rate is inevitable in small-size WTPs. Membrane process can be the best option for water treatment system in smart water grid because of the stable water quality regardless of variable flux (i.e. flux fluctuation), according to water demand [2]. In water treatment using freshwater source, the pollutant sizes of interest are in a range of one to several microns, which are much larger than the pore sizes (i.e. 0.01–0.1 μm) of microfiltration (MF) and ultrafiltration (UF) membranes [4–6]. Therefore, flux fluctuation has negligible effect on the turbidity of product water of MF/UF processes. However, it could increase membrane fouling because permeate flux is the key factor affecting fouling [4].

Fouling is one of the most important factors to design, construct, and operate a membrane system. The two key factors affecting MF/UF membrane fouling are feedwater quality and water flux through the membrane. Important water quality parameters for pilot-scale or real field MF/UF plants include turbidity, dissolved organic carbon (DOC), iron, manganese, and so forth. Turbidity stands for particulate matters, which play an important role to produce fouling layer (cake layer) on the membrane surface [7]. The cake layer composed of nano- and microparticles can be easily removed by backwash in a field application. The more severe sources of fouling in a field application are iron and manganese [8]. If these metallic ions are present in membrane feedwater, they can be precipitated to membrane pores as metallic oxide or hydroxide forms in oxidation condition and it is very difficult to clean these precipitates by backwash.

The effect of water flux on fouling is quite simple. Fouling becomes more severe as flux increases. If a membrane WTP is designed to accept periodic changes in water flux (i.e. flux fluctuation) to meet variable water demand for smart water grid, membrane will be more fouled at a higher flux and less fouled at a lower flux. But it is difficult to answer the question: Does the flux fluctuation make fouling worse or better than the general constant flux operation? The objective of this study is to answer this question. The best way to get the answer is to carry

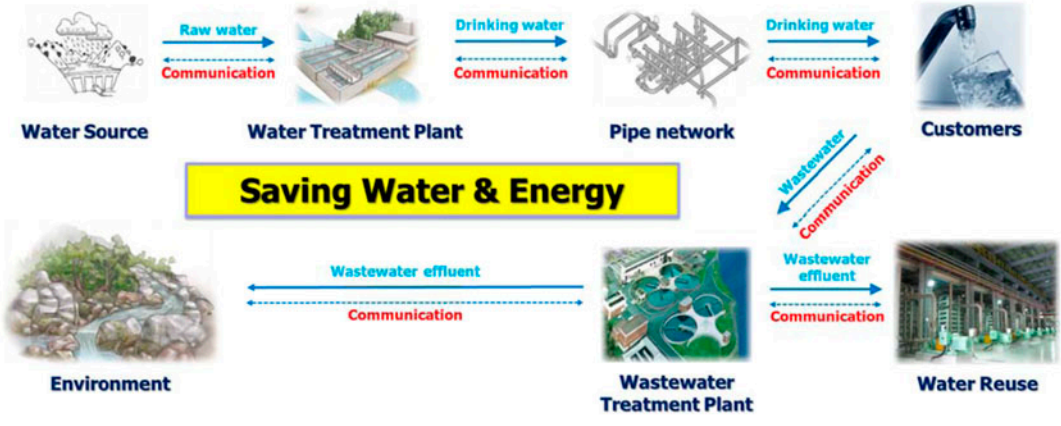

Fig. 1. Smart water grid: Water network with communication to save water and energy.

out a pilot- or full-scale test with two parallel units. Each unit should be operated with the flux fluctuation and the general constant flux operation modes, respectively. But this method needs a test period and cost to obtain the reasonable data. Therefore, we developed an MF/UF fouling model to be fitted to a real field condition. The model can reflect the complex fouling phenomenon including cake layer formation and pore blocking by particles and pore constriction by metallic ion precipitates. To obtain more reasonable simulation results, the fouling model was verified by pilot-scale MF plant data with commercial membrane modules (72 m^2 of membrane area). Instead of carrying out the real experiments that take long period and high cost, we simulated the various situations to identify the effect of flux fluctuation on the membrane fouling in a real field application.

2. Methods

2.1. MF Fouling model for field application

MF field application includes both filtration and backwash (or chemical-enhanced backwash) modes. In filtration mode, the permeate flux is maintained at a designed value. The permeate flux (J; m/s) can be expressed as a function of transmembrane pressure (TMP) (Δp; Pa), the dynamic viscosity of water (μ; Pa s), and the total resistance of membrane (R; m^{-1}) as depicted in Eq. (1).

$$J = \frac{\Delta p}{\mu R} \tag{1}$$

TMP increases as fouling occurs during the filtration mode in a constant flux MF operation. There were several mathematical fouling models according to fouling mechanisms and foulant characteristics [9–13] to describe changes in TMP. To reflect the complex fouling phenomenon in field application, we selected the simplest form of TMP equation [9] such as Eq. (2)

$$\frac{\mathrm{d}(\Delta p_i)}{\mathrm{d}t} = k(\Delta p_i)^n \tag{2}$$

where Δp_i is TMP (Pa) at ith filtration cycle, t is time (s), k is equation parameter (Pa^{1-n}/s), and n is fouling characteristic parameter ($n = 0$ for cake filtration, $n = 1.5$ for pore constriction, and $n = 2$ for complete blockage process as shown in Fig. 2 [14]). The parameters k and n in Eq. (2) can be obtained by a regression method using the TMP data according to the operation time for each filtration cycle, and the obtained value of n indicates the main mechanism of fouling in the field application.

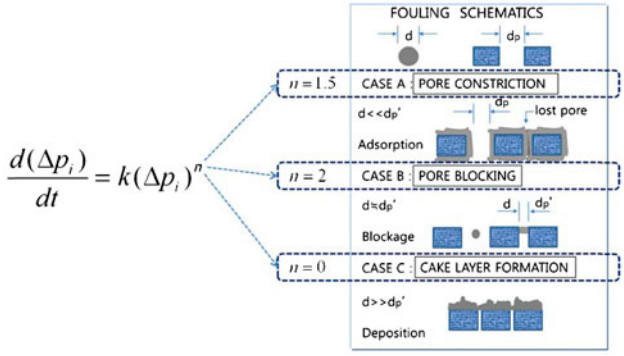

Fig. 2. Three fouling mechanisms related to the transmembrane pressure gradient equation.

Eq. (2) means that the increasing rate of TMP (i.e. the derivative of TMP with respect to time in Eq. (2)) becomes higher as TMP increases. It is also reasonable that the increasing rate of TMP becomes higher as the constant flux is designed to be a higher value, because TMP increases as fouling occurs and fouling becomes more severe as flux increases. Therefore, k should increase as the designed flux increases and it is assumed to be proportional to the designed permeate flux (J) for a constant flux operation as presented in Eq. (3).

$$k \propto J \tag{3}$$

The parameters, k and n, can be obtained by a regression method using the solution of the differential equation, Eq. (2), and operation data during a cycle of filtration mode.

The foulants accumulated during the filtration mode can be removed partially by normal backwash or chemical-enhanced backwash. This phenomenon is simulated using Eq. (4)

$$R_{i+1,0} = R_{i,0} + (R_{i,f} - R_{i,0}) \times \mathrm{RIF} \tag{4a}$$

$$\mathrm{RIF} \propto (R_{i,f} - R_{i,0})/R_{i,0} \tag{4b}$$

where $R_{i+1,0}$ and $R_{i,0}$ are total resistance of membrane at the beginning of $(i+1)$th and ith cycles, respectively, $R_{i,f}$ is total resistance of membrane at the end of ith cycle, and RIF is the ratio of irreversible fouling (i.e. the ratio of the remained fouling resistance after backwash ($= R_{i+1,0} - R_{i,0}$) to the fouling resistance during each cycle ($= R_{i,f} - R_{i,0}$) as shown in Eq. (4a)), which can be obtained using the method of least squares of errors with operation data. If backwash

efficiency is high, RIF becomes smaller. The three modeling parameters, k, n, and RIF are dependent upon the constant flux, foulant and membrane characteristics, pre-treatment type, backwash method (duration, frequency, and chemical use), and fouling mechanism.

2.2. MF pilot system

The MF fouling model discussed earlier has three fitting parameters (k, n, and RIF), which can be obtained using operation data. We used the operation data of MF pilot system with two commercial hollow fiber MF modules manufactured by Toray Industries, Inc. The system details are listed in Table 1 [15].

As listed in Table 1, the system was operated with dead-end filtration mode. Accumulated foulants during filtration were removed by periodic backwash. During backwash, sodium hypochlorite (NaOCl) was introduced to inhibit microbial growth and decrease biofouling potential. The amount of sodium hypochlorite was controlled to maintain 0.5 mg/l of residual chlorine concentration of backwash discharge water. Fig. 3 shows a picture of the MF pilot system and conceptual schematic of the MF module operation including filtration and backwash mode. The permeation velocity was designed as 1.0 m/d, and the backwash flux was 3.0 m/d.

During the operation period, the feed and permeate water quality parameters such as turbidity, DOC, iron and manganese were monitored using 2100 N Turbidimeter (Hach), TOC-V CPH (Shimadzu), and Atomic Absorption Spectroscopy AAnalyst 700 (Perkin Elmer).

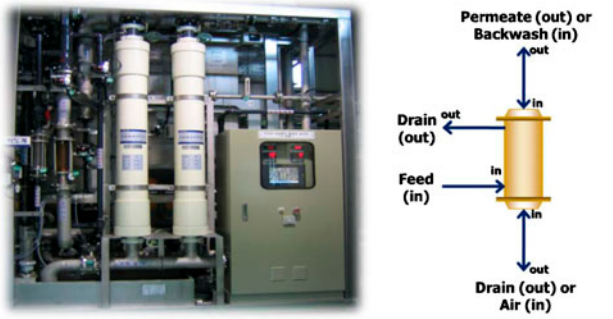

(a) Pilot plant (b) MF module operation

Fig. 3. The MF Pilot system.

3. Results and discussions

3.1. Water quality analysis

Feedwater and product water quality data for the MF pilot system is listed in Table 2 [15]. The operation condition is already discussed in Table 1. The main foulant in this system should be particulate matters because turbidity was removed clearly by MF operation. Iron and manganese might be the potent sources of fouling, because they can be precipitated to membrane surface and pores as metallic oxide or hydroxide forms in oxidation condition [8].

3.2. Verification of the MF fouling model

The MF fouling model was developed to quantify the effect of flux fluctuation on membrane fouling in field applicationTo verify the model, the field data from the MF pilot system were used. First, the

Table 1
The system details for the MF system for SWRO pre-treatment

Raw water		Reservoir water	Membrane type	MF
Operation type		Pressurized	Module type	Hollow Fiber
Filtration type		Dead end	Fiber diameter (mm)	1.5(outer)/ 0.9(inner)
Control type		Constant flux	Pore size (μm)	0.05
Cleaning Method	Backwash	Period: 30 min, Duration: 30 s (Normal backwash with aeration) + 30 s (Chemical-enhanced backwash)	Membrane Material	PVDF[a]
	CIP[b]	Acid: $(COOH)_2$ + HCl Base: NaOCl + NaOH	Membrane Area(m^2)	72 × 2 (EA)

[a]PVDF: polyvinylidene fluoride.
[b]CIP: cleaning in place.

Table 2
Raw water quality data in case of feedwater and product water

Parameters	Feedwater		Product water	
	Min	Max	Min	Max
Turbidity (NTU)	2	10	0	0.05
DOC (mg/l)	1.1	2.3	1.0	1.5
Fe (mg/l)	0.01	0.3	0.01	0.02
Mn (mg/l)	0.01	0.09	0.01	0.05

modeling parameters (k, n, and RIF) were determined using the field data. Then, we can produce TMP data according to operation time using the determined parameters.

Fig. 4 shows TMP data by modeling and field experiment for 100 days. Daily representative experimental data (i.e. one data per day) were taken to be presented in Fig. 4 for the clear comparison between the modeling and experimental data. The band observed in the modeling data in Fig. 4(a) means the increase in TMP during the filtration mode and the decrease in TMP during the backwash mode as presented in Fig. 4(b).

The modeling parameters n, k, and RIF were determined using the operation data of the first 20 days and the values are as shown in Eq. (5).

$$n = 0.9396 \tag{5a}$$

$$k = 8.12 \times 10^{-5} J \tag{5b}$$

$$\mathrm{RIF} = \frac{R_{i,f} - R_{i,0}}{R_{i,0}} \times 0.027 \tag{5c}$$

Since n is larger than zero and smaller than 1.5, the governing fouling mechanism is expected as both pore constriction ($n = 1.5$) and cake layer formation ($n = 0$). It can be inferred that turbidity is the main source of cake layer formation, and DOC, iron, and manganese are the main sources of pore constriction from the water quality analysis of feedwater and product water in Table 2. The produced modelling data (i.e. the simulation results) after 20th day of operation fit the experimental data very well as shown in Fig. 4. This means the three modeling parameters in Eq. (4) were realistic values and verified by the field experimental data.

3.3. Effect of flux fluctuation on membrane fouling

Using the realistic modeling parameters in Eq. (4), various MF simulation approaches were carried out. In each approach, the filtration time was 29 min and the backwash time was 1 min. Fig. 5 presents the

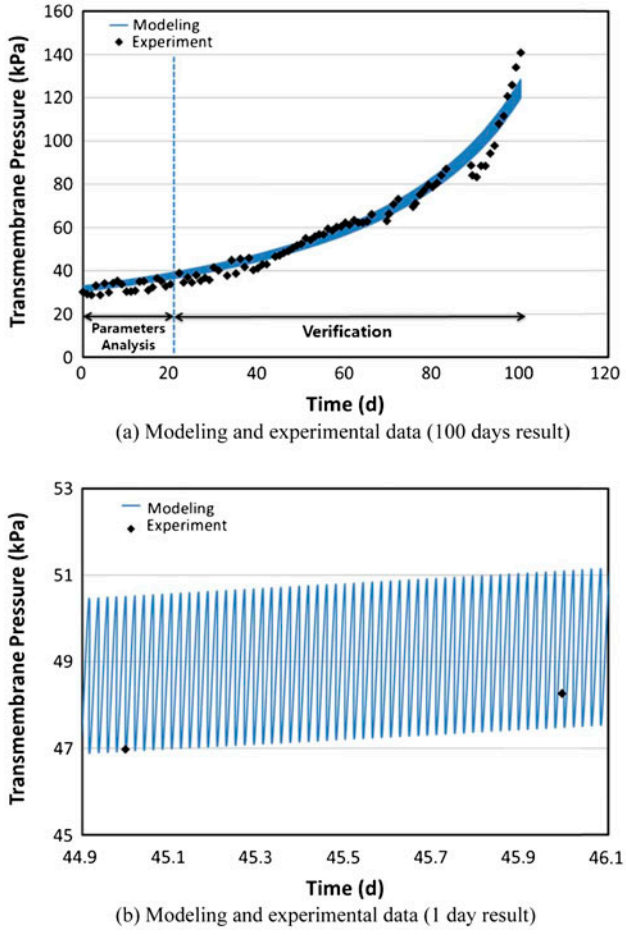

Fig. 4. Verification of the MF fouling model using pilot plant data.

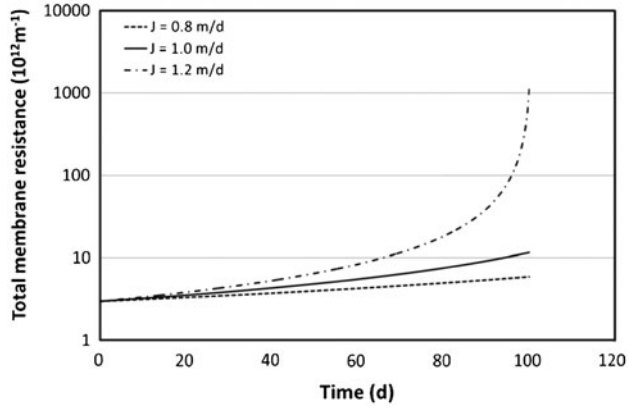

Fig. 5. Effect of permeate flux on the membrane fouling in the MF simulation.

effect of permeate flux on the membrane fouling in the MF simulation. Total membrane resistance was calculated using Eq. (1) with simulated TMP data and dynamic viscosity of water at 25°C assumed as a constant temperature in the simulation. To make a smooth line for each simulation, the total membrane resistance value at the end of each field cycle was removed. Therefore, the total membrane resistance shown in Figs. 5 and 6, is the sum of the intrinsic membrane resistance and the irreversible fouling resistance.

Total membrane resistance increased with the operation time, and the increasing rate became higher as the constant permeate flux increased from 0.8 to 1.2 m/d as shown in Fig. 5. When the constant flux increased from 1.0 to 1.2 m/d, the increase in total membrane resistance was much higher than the case when the constant flux changed from 0.8 to 1.0 m/d. This means the increase in the constant flux operation induces higher amount of fouling as the constant flux becomes larger. Therefore, we can imagine that the flux fluctuation (i.e. periodic changes in the constant flux), could harm MF operation in terms of fouling.

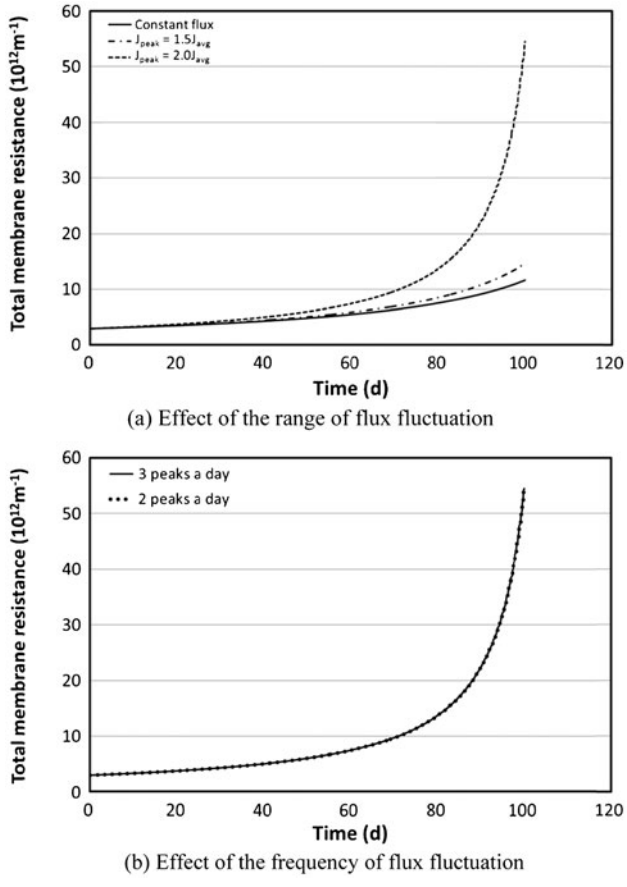

(a) Effect of the range of flux fluctuation

(b) Effect of the frequency of flux fluctuation

Fig. 6. Effect of flux fluctuation on membrane fouling in the MF simulation.

The effect of flux fluctuation on MF fouling is well described in Fig. 6. Three different cases for flux fluctuation were simulated, and the flux fluctuation pattern for each case is as follows:

(1) Case 1 ("$J_{peak} = 1.5J_{avg}$" in Fig. 6(a) and 2 peaks a day in Fig. 6(b)): Average flux = 1.0 m/d; J = 1.5 m/d for 6 h a day and J = 0.83 m/d for 18 h a day; two peaks a day (3-h duration per one peak)
(2) Case 2 ("$J_{peak} = 2.0J_{avg}$" in Fig. 6(a)): Average flux = 1.0 m/d; J = 2.0 m/d for 6 h a day and J = 0.66 m/d for 18 h a day; two peaks a day (3-h duration per one peak)
(3) Case 3 ("3 peaks a day" in Fig. 6(b)): Average flux = 1.0 m/d; J = 1.5 m/d for 6 h a day and J = 0.83 m/d for 18 h a day; three peaks a day (2-h duration per one peak)

As shown in Fig. 6(a), the increasing rate of total membrane resistance becomes higher in the case of flux fluctuation than that in the case of constant flux (no flux fluctuation), which means flux fluctuation does harm MF operation in terms of fouling. Fouling becomes more severe as the range of flux fluctuation increases while the average flux is maintained at a constant value as shown in Fig. 6(a). The frequency of flux fluctuation does not affect the membrane fouling if the average flux and the range of the flux fluctuation are not changed as shown in Fig. 6(b).

4. Conclusions

Flux fluctuation (i.e. periodic changes in the constant flux) is inevitable in membrane water treatment for smart water grid, where decentralized WTP should meet variable demand. In this study, the effect of flux fluctuation on the membrane fouling was quantified by using a simple and predictive MF fouling model for the field application. The fouling model was verified with operation data of a pilot-scale membrane WTP. From the simulation results using the verified model, the key findings can be drawn as follows:

(1) Even a small increase in permeate flux can make huge fouling effect during a long operation period as shown in Fig. 5.
(2) Flux fluctuation can induce higher fouling than the constant flux operation when the average flux is the same as the flux in the constant flux operation as shown in Fig. 6(a).
(3) Fouling becomes more severe as the range of flux fluctuation increases while the average flux

is maintained at a constant value as shown in Fig. 6(a).

(4) The frequency of flux fluctuation does not affect the membrane fouling if the average flux and the range of the flux fluctuation are not changed as shown in Fig. 6(b).

In conclusion, the range of flux fluctuation should be carefully selected when flux fluctuation in inevitable in membrane water treatment for smart water grid.

Acknowledgement

This research was supported by a grant (10CCTI-B056627-01-000000) from Construction Innovation Program funded by Ministry of Land, Transport, and Maritime Affairs of Korean government.

References

[1] M. Wissner, The smart grid—A saucerful of secrets? Appl. Energy 88 (2011) 2509–2518.
[2] N.S. Park, S.S. Kim, S.H. Chae, S. Kim, The effect of fluctuation in flow rate on the performance of conventional and membrane water treatment for a smart water grid, Desal. Water Treat. 47 (2012) 17–23.
[3] P. Gikas, G. Tchobanoglous, The role of satellite and decentralized strategies in water resources management, J. Environ. Manage. 90 (2009) 144–152.
[4] S. Kim, H. Park, Applicability assessment of sub-critical flux operation in crossflow microfiltration by modeling and experiment, J. Environ. Eng. ASCE 128 (2002) 335–340.
[5] S. Kim, H. Park, Effective diameter for shear-induced diffusion for characterizing cake formation in crossflow microfiltration at polydisperse conditions, J. Environ. Eng. ASCE 131 (2005) 865–873.
[6] S. Kim, N.S. Park, T. Kim, H. Park, Reaggregation of flocs in coagulation-crossflow microfiltration, J. Environ. Eng. ASCE 133 (2007) 507–514.
[7] S. Kim, M. Marion, B.H. Jeong, E.M.V. Hoek, Crossflow Membrane Filtration of Interacting Nanoparticle Suspensions, J. Membr. Sci. 284 (2006) 361–372.
[8] J.L. Lim, N.S. Park, S. Kang, C.H. Kim, S. Lee, S. Kim, Iron and manganese fouling in microfiltration as a pretreatment of seawater reverse osmosis processes, Desal. Water Treat. 33 (2011) 323–328.
[9] H.P. Grace, Structure and performance of filter media, AIChE J. 2 (1956) 307–315.
[10] C.C. Ho, A.L. Zydney, Transmembrane pressure profiles during constant flux microfiltration of bovine serum albumin, J. Membr. Sci. 209 (2002) 363–377.
[11] X. Sun, D.M. Kanani, R. Ghosh, Characterization and theoretical analysis of protein fouling of cellulose acetate membrane during constant flux dead-end microfiltration, J. Membr. Sci. 320 (2008) 372–380.
[12] S. Chellam, N.G. Cogan, Colloidal and bacterial fouling during constant flux microfiltration: Comparison of classical blocking laws with a unified model combining pore blocking and EPS secretion, J. Membr. Sci. 382 (2011) 148–157.
[13] D.C. Sioutopoulos, A.J. Karabelas, Correlation of organic fouling resistances in RO and UF membrane filtration under constant flux and constant pressure, J. Membr. Sci. 407–408 (2012) 34–46.
[14] D. Cha, H. Park, S. Kim, J.L. Lim, S. Kang, C.H. Kim, A statistical approach to analyze factors affecting silt density index, Desal. Water Treat. 45 (2012) 276–283.
[15] K-water, Development of high efficiency advanced drinking water treatment technologies for producing high quality drinking water, Report ID: KIWE-WRC-08-10, Korea Water Resources Corporation, Republic of Korea, 2008.